Mechanical behavior of mixtures of circular and rectangular 2D particles

E.-M. Charalampidou[*,†], G. Combe[*], G. Viggiani[*] and J. Lanier[*]

[*] *Grenoble Universités, Laboratoire 3S-R, B.P.53X, 38041 Grenoble, France*
[†] *Institute of Petroleum Engineering, Herriot Watt, Edinburgh, Scottland*

Abstract. This paper presents the results of experimental compression tests on a 2D granular material composed of a mixture of circular and rectangular rods. Numerical simulations of the tests, using a Discrete Element Method (Molecular Dynamics), successfully reproduce the experimental results. The results of the comparison between experimental and numerical results highlights the important role of the contact laws (especially the rolling resistance). A statistical study of the rotations of rectangular particles during compression (experimental and numerical) is carried out. The results of such study are finally compared to the predictions of continuum mechanics.

Keywords: 2D analogue granular material, plane strain compression, discrete element method, kinematics observations, continuum mechanics
PACS: 45.70.-n, 45.70.Cc, 45.70.Vn, 61.43.-j, 83.80.Fg, 81.05.Rm, 83.80.Fg

INTRODUCTION

A series of tests have been performed on a two-dimensional analogue granular material, composed of rods with circular and rectangular sections, in a special laboratory apparatus ($1\gamma 2\varepsilon$) that permits full control of plane deformations. The experimental results are compared with the results of numerical simulations performed using a DEM code. In this paper, we shortly describe the experimental and numerical procedures. Then, we present the results obtained and discuss the kinematics of the granular system as observed in the experiments and in the DEM computations.

EXPERIMENTAL AND NUMERICAL PROCEDURE

The experiments were performed on the shear apparatus $1\gamma 2\varepsilon$, which is fully described in [1, 2]. The 2D analogue material is enclosed by a frame having the shape of an initially rectangular parallelogram, whose sides can be shortened or elongated to apply normal strain in the horizontal and vertical directions (Fig. 1).

The material tested consist of an assembly of 0.06 m long wooden ash rods, either circular (with diameters $D_1 = 2.0 \cdot 10^{-2}$ m, $D_2 = 1.4 \cdot 10^{-2}$ m, $D_3 = 1.2 \cdot 10^{-2}$ m) or rectangular (R_1, with dimensions $l \times h = (5.5 \times 2.0) \cdot 10^{-2}\ m \times m$). The rods are hand-deposed in successive layers in the apparatus. The intergranular friction angle between rods is $\phi_\mu = 25.5^\circ \pm 2^\circ$, whereas friction angle between rods and steel plates of the frame can be neglected.

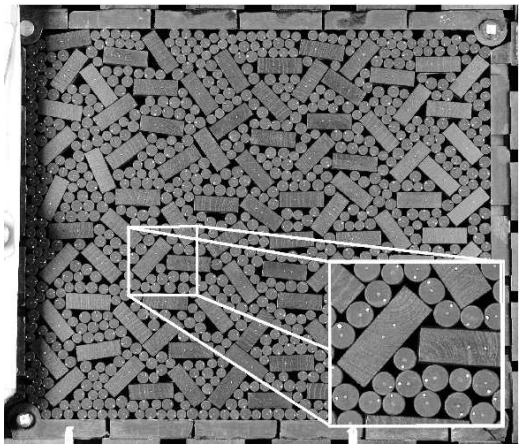

FIGURE 1. Sample CR-B3-50 in the $1\gamma 2\varepsilon$ apparatus. Sample size: $L_x \times L_y = 0.56m \times 0.47m$. Rectangular rods are specifically oriented at $\alpha = 0^\circ$ and $\alpha = \pm 45^\circ$.

The macroscopic behavior in terms of stress and strain is deduced from forces and displacements measured at the boundary. In addition, Digital Image Correlation of successive pictures of the deforming specimen allows to obtain the kinematics of each individual rod, see [3].

Four tests are considered herein: one on circular rods only (test *C-B1-50*) and three on mixtures of circular and rectangular particles (tests *CR-B1-50*, *CR-B2-50* and *CR-B3-50*), see table 1.The initial orientation of the rectangular rods was random in tests *CR-B1-50* and *CR-B2-50*, while in test *CR-B3-50* rectangles were placed at an angle $\alpha \simeq 0^\circ$ and $\alpha \simeq \pm 45^\circ$, see figure 1 and polar histograms in figure 2.

Two dimensional numerical simulations were carried

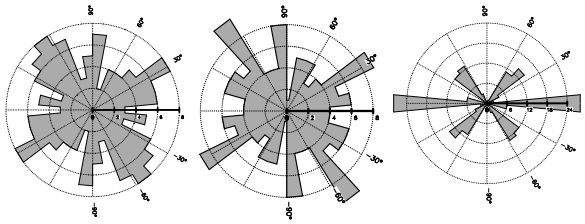

FIGURE 2. Histograms of rectangular rods orientation for *CR-B1-50* to *CR-B3-50* samples (from left to right) under an isotropic loading (50 kPa). Histograms are computed with 17 classes over $[-90,90]$ degrees range.

TABLE 1. Tested specimens

test	**Number of rods:** D_1, D_2, D_3, R_1
C-B1-50	415, 420, 423, 0
CR-B1-50	0, 420, 423, 89
CR-B2-50	0, 420, 422, 89
CR-B3-50	0, 420, 423, 95

out using the discrete element method within the framework of molecular dynamics (MD) [4]. Grains interact at their contacts with a linear elastic law, a Coulomb friction and a rolling resistance law. The normal contact force f_n is related to the normal interpenetration (or overlap) h of the contact as $f_n = k_n \cdot h$, with f_n vanishing if the contact disappears. The tangential component f_t of the contact force is proportional to the tangential elastic relative displacement, with a tangential stiffness coefficient k_t. The Coulomb condition $|f_t| \leq \mu f_n$ requires an incremental evaluation of f_t at every time step, which leads to some amount of slip each time one of the equalities $f_t = \pm\mu f_n$ is imposed (μ corresponds to the contact friction coefficient). The actual $1\gamma 2\varepsilon$ experiments suggest that the 2D contact lengh between the rods is larger that a simple contact point. Therefore, a third contact law is considered in the simulations, which takes into account some contact rolling resistance. Following a suggestion by [5, 6], the moment M transmitted by a particle to another is proportional to the relative rotation $\Delta\omega$ through a rotational stiffness k_r. As for rotational resistance, its absolute value cannot exceed μ_r.

Assuming that normal contact forces are always proportional to h, our contact detection is able to take into account three kinds of intergranular contacts: contacts between discs, contacts between a disc and a rectangle and contacts between rectangles. Contact detection and forces computation between rectangles do not use classical methods based on the area overlap between polygons [8]. Instead, we use the *shadow overlap* technique proposed by J.-J. Moreau [9] and adapted to our MD approach. Finally, the motion of grains is computed by solving Newton's equations which use a third-order predictor-corrector discretization scheme [7]. Numerical assemblies of discs and rectangles are generated from digitalized positions (and orientations) of wooden rods of experimental samples. Following the actual $1\gamma 2\varepsilon$ tests, the first computational step is an isotropic compression up to $p = 50$ kPa. Since the actual rods have a length $L = 0.06$ m and a normal stiffness $k_n \simeq 5 \cdot 10^7$ N/m, the stiffness level of grain contact is $\kappa = \frac{k_n}{pL} = 1000$ [10]. Note that the inverse of parameter κ can be interpreted as the mean level of contact deformation ($1/\kappa$). Tangential stiffness k_t is taken equal to the normal stiffness k_n. Finally, assuming that $l = 1$ mm is the contact length, rotational stiffness $k_r = k_n \times l^2$. Following [6], we assume the rolling resistance threshold $\mu_r = \mu \times l$.

MECHANICAL RESPONSE UNDER VERTICAL COMPRESSION

All tests started with isotropic compression to 50 kPa. Then, vertical compression was applied under strain control, while the horizontal stress σ_x was kept constant. Axial strain rate $\dot{\varepsilon_y}$ was equal to $10^{-3}\ s^{-1}$ and $\dot{\varepsilon_y} = 10^{-2}\ s^{-1}$ for MD simulations. Stress strain responses are shown in figure 3 in term of stress ratio $\eta = (\sigma_y - \sigma_x)/(\sigma_y + \sigma_x)$ vs. vertical strain ε_y. Large η fluctuations are observed, which is typical of 2D granular materials, especially when the number of grains is relatively small (e.g., [12]). It appears that *C* and *CR* specimens exhibit very similar responses, i.e., rectangles do not seem to have a clear influence on the macroscopic behavior. This suggests that the mechanical behavior of the mixtures is likely governed solely by the particles in greater proportion, i.e. the circular grains. Note that the highest shear resistance is shown by specimen *CR-B1-50* where rectangles are randomly oriented. As a synthesis of the observed mechanical behaviors, table 2 gives some estimations of the angle ϕ which corresponds to the macroscopic friction angle associated to the maximum shear strength. In order to quantify the sample dilatancy, we introduce here the dilatancy angle which is classically calculated by the following expression: $\frac{d\varepsilon_v}{d\varepsilon_y} = \frac{-2\sin\psi}{1-\sin\psi}$, where ε_v is the volumetric strain. For each tests, ψ is computed in the linear increasing part of the volumetric curve. Test *CR-B2-50* shows a peculiar response, in that both dilatancy and shear strength are definitely lower than the other three tests. This is likely due to the fact that this test was actually subjected to some deviatoric loading-unloading before isotropic compression. Even if the specimen was handshaked before isotropic compression, it appears that the effect of this previous loading history was not completly erased.

Numerical simulations were carried out of the three

TABLE 2. Friction and dilatancy values

Test	ϕ (degrees)	ψ (degrees)
C-B1-50	30.5	21.7
CR-B1-50	34	21.4
CR-B2-50	27.5	11.9
CR-B3-50	30.8	20.2

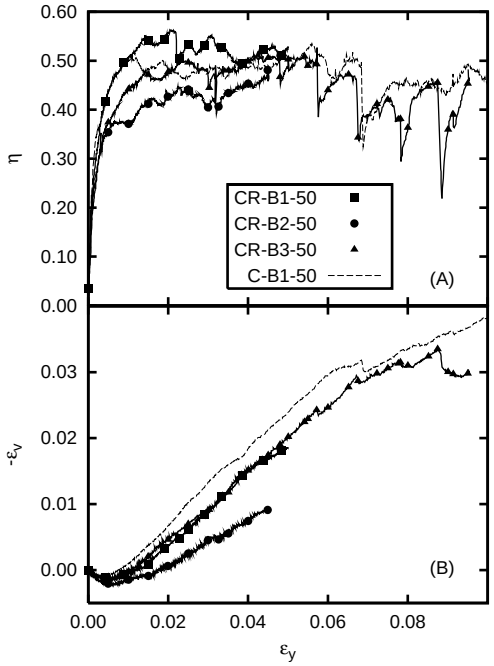

FIGURE 3. Stress-strain experimental responses. (A) stress ratio vs. vertical strain. (B) volumetric strain vs. vertical strain.

tests on the mixtures. For each numerical test, the initial distribution of rectangular and circular particles was the same as in the corresponding actual $1\gamma 2\varepsilon$ test. This was directly obtained by the digital image of the initial configuration of the specimen. Numerical and experimental results are compared in figure 4. If we assume no rolling resistance between grains ($\mu_r = 0$), then the numerical behavior at moderate and large strain is subsantially different from the experimental one. In particular, a lower shear strength is observed. At low vertical strain (i.e., close to the isotropic state), numerical and experimental results are very close to each other. Since the mechanical behavior close to the isotropic state is governed by contact elastic properties, this indicates that the chosen stiffness level of grain contact κ is appropriate. When the rolling resistance is taken into account ($\mu_r \neq 0$), the numerical results are close to the experimental one, except for ε_v of test *CR-B2-50* for which the experimental loading history is peculiar (as previously explained). Nevertheless, figure 4 also indicates that rolling resistance has hardly any effect on the volumetric behavior.

PARTICLES KINEMATICS

In continuum mechanics, the rotation $\Delta\alpha$ of a material direction initially inclined of an angle α with respect to the horizontal is given by [11]:

$$\Delta\alpha = -\frac{\gamma}{2} + \frac{\varepsilon_y - \varepsilon_x}{2}\sin 2\alpha + \frac{\gamma}{2}\cos 2\alpha \qquad (1)$$

where ε_x and ε_y are the horizontal and vertical strain, respectively, while γ is the shear strain ($\gamma = 0$ for a vertical compression test). If the rectangular rods in a $1\gamma 2\varepsilon$ sample are regarded as material lines, then the above equation can be used to predict their rotation (under the assumption that the strain in the sample is homogeneous). Such continuum mechanics based predictions are compared in Fig. 5-(A) to the rotations that were actually measured in the experiments. Experimental data in this figure come from tests *CR-B1-50*, *CR-B2-50* and *CR-B3-50*, and correspond to values measured by DIC upon a (vertical) strain increment of about 4 %. All rectangles rotations are averaged by classes of 12°. The comparison indicates that there is a large scatter, but the average values of measured rotations are very close to those predicted by continuum mechanics[1].

Rectangles rotations predicted by eq. (1) can be also compared to those obtained by DEM simulations of vertical compression tests on numerical samples. Data in Fig. 5-(B) come from over 30 such tests performed on samples with an initial particles configuration close (but not coincident) to that of samples *CR-Bx-50*. Each numerical sample was generated by randomly replacing some of the original circular particles (with diameters D_2 and D_3, see Table 1) by slightly smaller particles (with diameters $D_2^{'}$ and $D_3^{'}$ in between 80% and 100% of D_2 and D_3, respectively). As for the experimental data, the comparison indicates that there is a large scatter, but the average values of rectangles rotations obtained in the DEM numerical tests are very close to those predicted by continuum mechanics ($TNS = 0.75$).

Finally, numerical simple shear tests (with $\gamma = 10$ degrees) were also performed on the DEM samples. As for the case of vertical compression, the results (shown in Figure 5-(C)) indicate that the rotation of the rectangular particles averaged by 15 classes of 12° is fairly well predicted by continuum mechanics ($TNS = 0.71$).

[1] A synthetic measure of such an agreement is provided by the so-called *Nash-Sutcliffe efficiency coefficient* (*TNS*) [13]. *TNS* is a scalar quantity varying from 0 to 1, the latter value indicating a perfect agreement. For the comparison in Fig. 5-(A), TNS = 0.88.

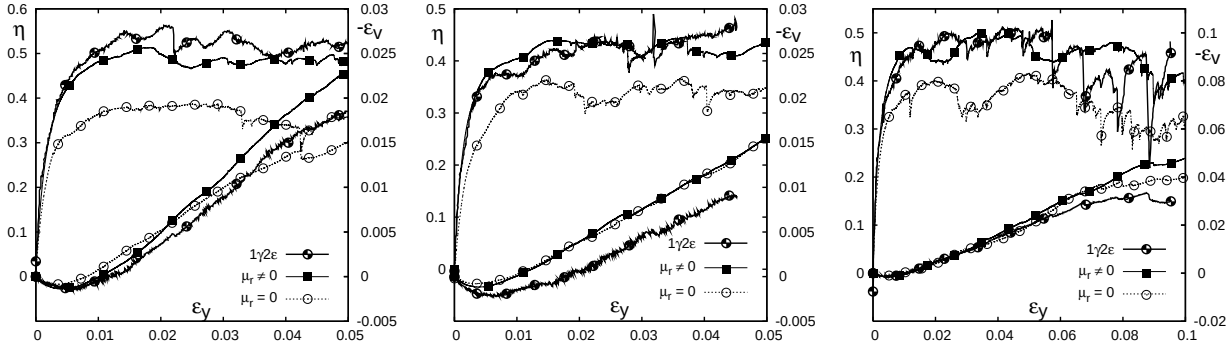

FIGURE 4. Comparison of the macroscopic behavior between experimental (bold curve) and *MD* results (thin and dashed curves) for *CR-B1-50* to *CR-B3-50* samples (from left to right). Influence of rolling resistance μ_r.

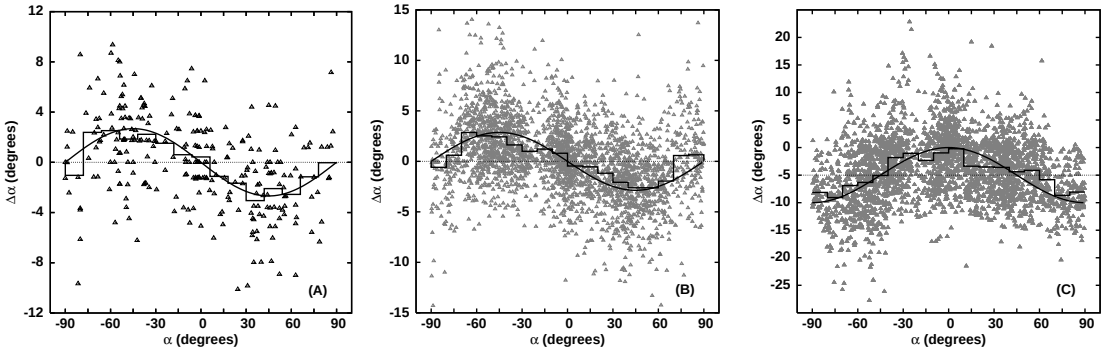

FIGURE 5. Rotation $\Delta\alpha$ of rectangular rods as a function of their initial orientation α. Statistics on data points (one per rectangle) provide histograms of rotations computed over 15 classes of 12 degrees. Bold curves are the rotations given by continuum mechanics, eq. (1). (A) *CR-Bx-50* $1\gamma2\varepsilon$ samples, 273 rectangular rods. $\langle\varepsilon_y\rangle = -0.0388$ and $\langle\varepsilon_x\rangle = 0.0554$. (B) *CR-By-50* DEM samples, 2730 rectangles. $\varepsilon = [\varepsilon_x;0;0;\varepsilon_y]$, $\varepsilon_x = -\varepsilon_y = 0.05$. (C) *CR-By-50* DEM samples, 2730 rectangles. $\varepsilon = [0;\gamma/2;0;0]$, $\gamma = 10^\circ$.

CONCLUSIONS

Based on the results obtained in this study, the following conclusions can be drawn:

- The rotation of individual rectangular particles is largely scattered, which is not surprising [2]. However, their average rotation conforms very well to the rotation predicted by continuum mechanics for homogeneous strain, which is not at all an obvious result.

- rolling contact resistance has a remarkable influence on the stress-strain response of granular materials. Provided such a resistance is properly taken into account, our DEM is capable of accurately reproducing the experimentally observed behavior of mixtures of circular and rectangular 2D particles.

REFERENCES

1. Joer H., Lanier J., Desrues J., Flavigny E. *Geotech Test J* Vol: 15(2) 129–137, 1992
2. Calvetti F., Combe G., Lanier J. *Mech Co-Fric Mat* Vol 2, 121–163, 1997
3. Sibille L., Froiio F. *Granular Matter* Vol: 9 183–193, 2007
4. Cundall P.A., Strack O.*Géotechnique* Vol: 29(1) 47–65, 1979
5. Iwashita K., Oda M. *J Eng Mech-ASCE*, vol 124(3), 285–292, 1998
6. Gilabert F.A., Roux J.-N., Castellanos A. *Phys Rev E*, Vol 75, 011303, 2007
7. Allen M.P. and Tildesley D.J. "Computer simulation of liquids" *Oxford Science Publications*, Oxford, 1987
8. Alonso-Marroquin F., Luding S., Herrmann H. J., Vardoulakis I. *Phys Rev E* Vol 71, 051304, 2005
9. Saussine G., Cholet C., Gautier P.-E., Dubois F., Bohatier C., Moreau J.-J. *Comput Method Appl M* Vol: 195(19-22) 2841–2859, 2006
10. Roux J.-N., Combe G. *C.R. Physique* 3, 131–140, 2001
11. Combe G., Charalampidou E.-M., Viggiani G., Lanier J. *To be submitted to Granular Matter*
12. Evesque P., Meftah W., Biarez J. *CRAS*, Vol 316, 321–327, 1993
13. Nash J.E., Sutcliffe J.V. *J Hydrol*, vol: 10(3), 282–290, 1970